Acta Crystallographica Section D
**Biological Crystallography**
ISSN 0907-4449

# Purification, N-terminal sequencing, crystallization and preliminary X-ray diffraction analysis of atratoxin, a new short-chain α-neurotoxin from the venom of *Naja naja atra*

**Xiongying Tu,[a,b] Qingqiu Huang,[a,b] Xiaohua Lou,[a,b] Maikun Teng[a,b]† and Liwen Niu[a,b,c]*†**

[a]Key Laboratory of Structural Biology, University of Science and Technology of China, CAS, 96 Jinzhai Road, Hefei, Anhui 230026, People's Republic of China, [b]Department of Molecular and Cell Biology, School of Life Sciences, University of Science and Technology of China, 96 Jinzhai Road, Hefei, Anhui 230026, People's Republic of China, and [c]National Laboratory of Macromolecules, Institute of Biophysics, CAS, 15 Datun Road, Beijing 100101, People's Republic of China

† Both these authors would like to be considered as corresponding authors.

Correspondence e-mail: lwniu@ustc.edu.cn

Received 19 October 2001
Accepted 7 February 2002

Atratoxin, a new α-neurotoxin purified to homogeneity by a series of liquid chromatographies from the venom of *Naja naja atra* (mainland Chinese cobra), is a small single-polypeptide alkaline protein with a pI of about 9.5 and molecular weight of 6952 Da estimated by mass spectrometry. Although the sequencing of the N-terminal 15 residues (LECHNQQTTQQPEGG) shows that this neurotoxic protein contains most of the residues, especially at the conserved positions, of the consensus sequence of short-chain α-neurotoxins, the natural mutations in the N-terminal Loop-1 presented by the sequence alignment may have structural or functional implications for the interactions between α-neurotoxins and related receptors. Single crystals of atratoxin have been grown from drops containing the necessary $Cu^{2+}$ ions by the conventional hanging-drop vapour-diffusion method. The crystals diffract X-rays to 1.6 Å resolution and belong to space group $C222_1$, with unit-cell parameters $a$ = 47.36, $b$ = 47.83, $c$ = 91.31 Å, corresponding to a volume-to-mass ratio of 1.85 Å$^3$ Da$^{-1}$ and two molecules in each asymmetric unit.

## 1. Introduction

More than 100 α-neurotoxins from snake venoms have been sequenced. These can be classified into the short-chain α-neurotoxins (60–62 amino-acid residues and four disulfide bonds) and the long-chain α-neurotoxins (65–74 amino-acid residues and five disulfide bonds) (Juan *et al.*, 1999; Tsetlin, 1999). These proteins specifically target nicotinic acetylcholine receptors (nAChRs) located in the neuron–muscle junction and block signal transmission from the motor nerve ending to the muscle, leading to death from asphyxiation (Tu, 1973). The α-neurotoxins are of use in medicine, having a high specificity for particular subtypes of receptors. The expanding neurotoxin library serves as a powerful tool to detect the subtle pharmacological differences between different nAChRs (Endo & Tamiya, 1987; Changeux & Edelstein, 1998) and also provides templates for modelling new drugs or mimics with the desired pharmacological properties (Le Du *et al.*, 2000; Harvey *et al.*, 1998).

According to structural analysis reports by X-ray crystal diffraction or NMR, the single polypeptide of α-neurotoxins folds into a topological feature of three loops protruding from a core formed by four or five disulfide bonds, just like fingers from a palm (Endo & Tamiya, 1987; Betzel *et al.*, 1991); thus, the α-neurotoxins share a very similar and comparable three-dimensional scaffold and belong to the superfamily of three-finger proteins. It is already known that the high affinity and specificity of neurotoxins for nAChRs results from interactions of 'multi-attachment point character' (Tsetlin *et al.*, 1982; Martin *et al.*, 1983; Patricio *et al.*, 1999). As there is as yet no structural information available for complexes of α-neurotoxins and nAChRs, the structural basis that accounts for the role of the important residues which distinguish α-neurotoxins of similar three-dimensional structures from their relatives is still unclear. In order to obtain further insight into the structure–function relationships of the various snake-venom α-neurotoxins, an effective method is to undertake further structural analyses and comparison of different α-neurotoxins. There are several structural models of short α-neurotoxins available in the PDB (Corfield *et al.*, 1989; Nastopoulos *et al.*, 1998; Smith *et al.*, 1998; Saludjian *et al.*, 1992; Gaucher *et al.*, 2000; Tsernoglou & Petsko, 1976; Hatanaka *et al.*, 1994; Yu *et al.*, 1993; Zinn-Justin *et al.*, 1992; Brown & Würich, 1992), but no X-ray structures of short-chain α-neurotoxins from cobra venoms have yet been reported. This paper describes the isolation, sequencing of N-terminal residues, crystallization and preliminary X-ray diffraction of atratoxin, a new short-chain α-neurotoxin from the venom of *N. naja atra* (mainland Chinese cobra).

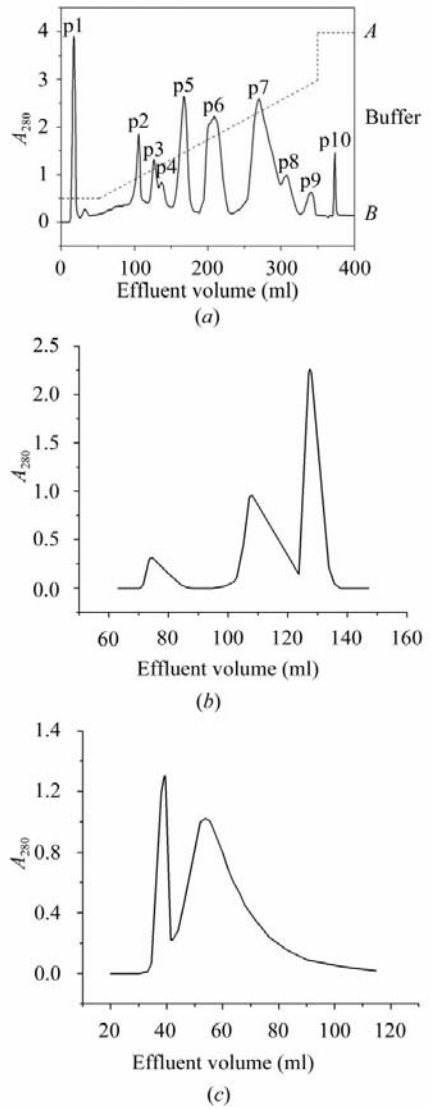


**Figure 1**
(*a*) CM-Sepharose chromatography. 0.5 g of dried crude venom was dissolved in 10 ml 0.02 *M* $NaH_2PO_4$–$Na_2HPO_4$ pH 6.0 (buffer *A*) at 277 K overnight, centrifuged at 10 000*g* to remove insoluble materials and then applied to a CM-Sepharose column (1 × 20 cm) pre-equilibrated with the same buffer. At a flow rate of 1 ml $min^{-1}$, the column was first eluted with 200 ml buffer *A*, then with a pH and salt gradient produced by mixing 200 ml of buffer *A* with 200 ml 0.5 *M* NaCl, 0.02 *M* $Na_2HPO_4$–$NaH_2PO_4$ pH 8.0 (buffer *B*) and finally with two column volumes of buffer *B*. The fraction corresponding to peak 5 was pooled and concentrated for further gel filtration. (*b*) Superdex 75 gel filtration. The peak 5 fraction from the previous CM-Sepharose chromatography was applied to a Superdex 75 column pre-equilibrated with 0.02 *M* Tris–HCl pH 8.0 containing 0.3 *M* NaCl. The column was eluted with the same buffer at a rate of 42 ml $h^{-1}$. The last fraction was pooled and concentrated for further purification. (*c*) Hydrophobic interaction chromatography. The concentrated protein solution from the Superdex 75 column was equilibrated by dialyzing against 2 *M* $(NH_4)_2SO_4$ and then applied to a phenyl Sepharose 6 Fast Flow column (1 × 30 cm) pre-equilibrated with 2 *M* $(NH_4)_2SO_4$. The column was directly washed with the equilibrium solution at a flow rate of 30 ml $h^{-1}$. The last fraction was pooled, desalted and lyophilized.

## 2. Materials and methods

### 2.1. Materials

Dried crude venom of the mainland Chinese cobra was obtained from the southern mountain region of Anhui Province, China. CM-Sepharose, Superdex 75 and phenyl Sepharose 6 Fast Flow were purchased from Pharmacia (Uppsala, Sweden). Sodium dodecyl sulfate (SDS) and ampholytes were produced by Fluka Co. Ltd (Switzerland) and the Chinese Military Medical Academy, respectively. Sodium chloride, sodium acetate, glacial acetic acid and ethanol were purchased from Shanghai Chemical Reagent Co. Ltd. Other regents and chemicals were of analytical grade from commercial sources.

### 2.2. Protein purification

The isolation of atratoxin samples for crystallization and characterization was carried out by three-step chromatography. A CM-Sepharose column was first utilized to isolate the crude venom (see Fig. 1*a*). A Superdex 75 column was then used to purify the protein fraction containing atratoxin from the first chromatographic step (see Fig. 1*b*). Finally, hydrophobic interaction chromatography was performed as the final purification (see Fig. 1*c*). The purified samples were desalted and lyophilized for subsequent crystallization and characterization. The purity was assayed by SDS–PAGE with and without the reducing agent DTT (see Fig. 2).

### 2.3. Estimation of molecular weight and isoelectric point

The molecular weight of the purified protein was estimated by MALDI-TOF (see Fig. 2) on a Bruker BIFLEX mass spectrometer using sinapinic acid as the matrix (Beavis & Chait, 1990) and the method of sample preparation described by Martin de Llano *et al.* (1993). The isoelectric point was estimated by isoelectric focusing (IEF) on an ampholine polyacrylamide slab gel using pH 3–9.5 ampholytes following the instructions of the manufacturer.

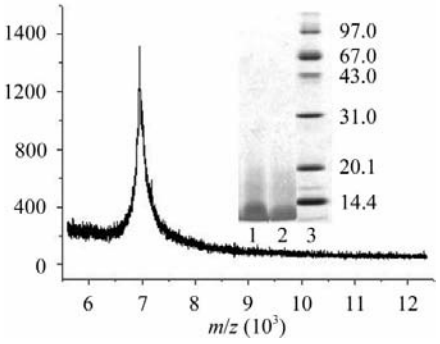


**Figure 2**
Mass-spectrometric estimation of the molecular weight of atratoxin. Inset, SDS–PAGE of atratoxin. Lanes 1 and 2 are samples under non-reducing and reducing conditions, respectively. Lane 3, protein standards (molecular weights are given in kDa).

### 2.4. Crystallization and preliminary X-ray diffraction analysis

The lyophilized protein was dissolved in double-distilled water, adjusted to a concentration of 20 mg $ml^{-1}$ and then centrifuged to remove insoluble materials before crystallization. The crystals were grown at room temperature (about 298 K) by the vapour-diffusion method using tissue-culture plates and siliconized glass cover slips. After no positive results were obtained using Crystal Screen and Crystal Screen II, the initial crystallization conditions were determined by screening combinations of different types of precipitants (such as ethanol, PEG series *etc.*) with a series of pH values (4.6, 5.6, 6.5, 7.0, 8.0, 8.5, 9.0 *etc.*). On mixing 2 µl protein solution with 2 µl precipitant solution containing 2.5 *M* NaCl and 10% ethanol buffered with 0.1 *M* NaOAc–HOAc at pH 4.6, needle-shaped crystals

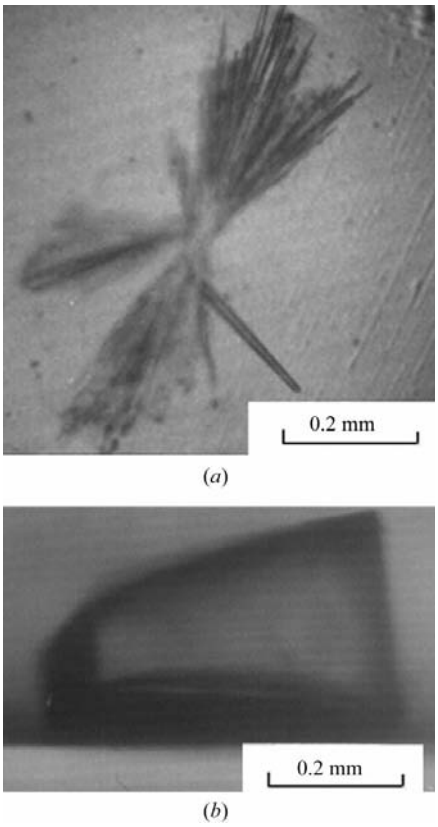


**Figure 3**
Crystals of atratoxin grown (*a*) in the absence of $Cu^{2+}$ ions and (*b*) in the presence of $Cu^{2+}$ ions.

**Table 1**
Data collection and reduction statistics.

Values in parentheses are for the highest resolution shell (1.64–1.61 Å).

| | |
|---|---|
| Space group | $C222_1$ |
| Unit-cell parameters | |
| $a$ (Å) | 47.36 |
| $b$ (Å) | 47.83 |
| $c$ (Å) | 91.31 |
| Resolution range (Å) | 16.83–1.61 |
| Observations | 69609 |
| Independent reflections | 12884 |
| $R_{\rm merge}$† (%) | 6.1 (15.4) |
| Completeness‡ (%) | 93.3 (86.9) |

† $R_{\rm merge} = \sum_h \sum_j |I(h)_j - \langle I(h)\rangle| / \sum_h \sum_j I(h)_j$, where $I(h)_j$ is the observed intensity of the $j$th reflection and $\langle I(h)\rangle$ is the mean intensity of reflection $h$. ‡ Completeness is the ratio of the number of observations to the number of possible reflections.

(Fig. 3*a*) appeared one week later. After investigating different additive agents and protein concentrations, it was found that 10 m*M* $Cu^{2+}$ significantly improved the crystal quality. Crystals of dimensions 0.4 × 0.2 × 0.2 mm (Fig. 3*b*) were finally obtained using the following procedure: 4.5 µl of protein solution was mixed with an equal volume of precipitant solution containing 2.5 *M* NaCl, 10% ethanol and 10 m*M* $CuCl_2$ buffered with 0.1 *M* NaOAc–HOAc at pH 4.6 and then equilibrated against 450 µl of the same precipitant solution.

The diffraction data were collected at room temperature from a single crystal using a MAR Research imaging plate (diameter 300 mm) mounted on an X-ray generator with a graphite monochromator and a sealed copper-target tube. The voltage and current of the working tube were 50 kV and 50 mA, respectively. A total of 95 imaging frames were recorded at a crystal-to-detector distance of 110 mm, an oscillation angle of 1° and an exposure time per image frame of 420 s (Fig. 4). Data processing was performed using the program *marFLM* (Bartels & Klein, 2000). The self-rotation function was calculated and analyzed using the program *POLARRFN* from the *CCP*4 suite (Collaborative Computational Project, Number 4, 1994). The final statistics for data collection and reduction are summarized in Table 1.

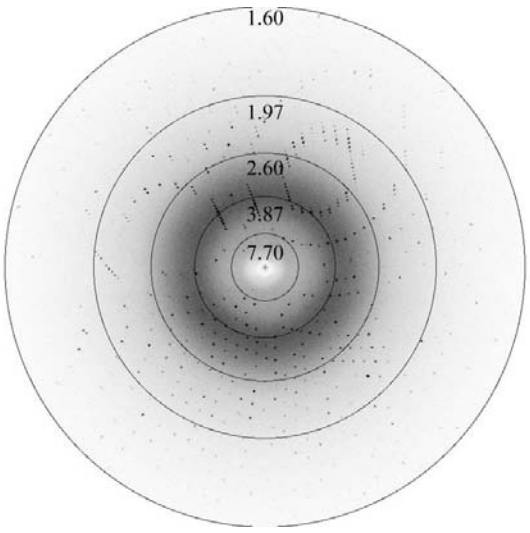


**Figure 4**
A diffraction pattern from an atratoxin crystal.

### 2.5. Sequencing of N-terminal amino-acid residues

The protein produced from the chromatography was further purified by crystallization under conditions containing 2 *M* NaCl and 10% ethanol buffered with HOAc–NaOAc at pH 4.6. The crystals were picked up into a clean Eppendorf tube, centrifuged and washed twice using the reservoir liquid and then dissolved in double-distilled water and desalted. Sequencing of the N-terminal amino-acid residues was performed by Edman degradation with an Applied Biosystems 476A Protein Sequencer at Hunan Normal University, China.

## 3. Results and discussion

Atratoxin, purified to homogeneity by a series of liquid chromatographic steps from the venom of *N. naja atra*, is a small single-polypeptide alkaline protein with a pI of about 9.5 (experimental data not shown). The purified protein appears as a single band on SDS–PAGE gel under both reducing and non-reducing conditions (see Fig. 2) and shows only one molecular-weight peak of 6952 Da in the mass spectrum (see Fig. 2).

The accumulating sequence data for short-chain α-neurotoxins allow us to map their consensus sequence and generalize their characteristic features. Sequencing of the N-terminal 15 residues of atratoxin shows that this protein contains most of the residues, especially at the conserved positions in the N-terminal loop, of the consensus sequence of short-chain α-neurotoxins: LECHNQQTTQ-QPEGG, with the typical N-terminal sequence LECHNQQ and residue repetitions (*e.g.* QQ, TT, QQ and GG). In combination with the estimated molecular weight, this sequence alignment strongly indicates that atratoxin should be classified as a new member of the family of short-chain α-neurotoxins. However, attention should be paid to the differences presented by the comparison. For example, the residues at positions 13, 14 and 15 are substituted by one Glu residue and two Gly residues; the two Ser residues at sites 8 and 9 are displaced by two Thr residues. These natural mutations may have structural or functional implications for the interactions between α-neurotoxins and related receptors.

The crystallized atratoxin has been confirmed as belonging to the orthorhombic crystal system, with space group $C222_1$ and unit-cell parameters $a$ = 47.36, $b$ = 47.83, $c$ = 91.31 Å. Based on the molecular weight and the unit-cell volume, two molecules of atratoxin are present in each asymmetric unit, corresponding to a volume-to-mass ratio of 1.85 $Å^3\ Da^{-1}$ (Matthews, 1968). Calculation and analysis of the self-rotation function shows that a non-crystallographic twofold axis exists in the asymmetric unit (data not shown), *i.e.* the protein molecules associate into a dimer after crystallization.

It is believed that the mechanism of the binding of neurotoxins to receptors involves intermolecular hydrogen bonding of the β-sheet in Loop-3, which is part of the three-stranded β-sheet (Betzel *et al.*, 1991; Brown & Würich, 1992). For long-chain neurotoxins such as α-cobrotoxin and α-bungarotoxin, auto-dimerization through this intermolecular β-sheet association has been observed in both crystal and solution structures. Although such dimerization has not been observed for short-chain neurotoxins in solution, the exposed edge of such a three-stranded β-sheet could clearly be observed. Recently, dimeric crystal structures of erabutoxin-b and erabutoxin-a from sea snake have been determined (Saludjian *et al.*, 1992; Nastopoulos *et al.*, 1998). They exhibit dimeric association through the parallel β-sheet around the non-crystallographic twofold axis. The structure determination of atratoxin from cobra will provide further evidence that this mechanism of intermolecular interaction also exists in the short-chain neurotoxin subclass. Interestingly, the atratoxin crystal appears blue in colour, indicating that $Cu^{2+}$ ions may be present in the crystal, although no $Cu^{2+}$ ions were detected in the non-crystalline samples (experimental data not shown). Considering that the addition of $Cu^{2+}$ ions effectively changed the crystal form from twinned needles to a single block, $Cu^{2+}$ ions may play a role in stabilizing the molecular conformation; however, it is still

unclear whether or not $Cu^{2+}$ ions can induce dimerization and further evidence needs to be accumulated, as no relevant report has yet been published of the binding of $Cu^{2+}$ ions to neurotoxins.

The space group of the atratoxin crystal is different from those of the erabutoxins, which belong to space group $P2_12_12_1$, *i.e.* the two kinds of proteins might possess different close-packing modes after crystallization. Structural comparison of atratoxin with other short-chain neurotoxins will show the conformational changes of the residues, particularly those in the functional regions, and will provide further knowledge of the mechanism by which short-chain neurotoxins sense the subtle differences in the receptors. The sequencing of all amino-acid residues in atratoxin and the structural determination are being undertaken in our group, which will not only solve the questions mentioned above, but will also provide deeper insight into the structure–function relationship of $\alpha$-neurotoxins.

Financial support for this project to LN and MT was provided by research grants from the National Natural Science Foundation of China (Grant Nos. 39870108 and 30025012.), the 973 Plan of the Ministry of Science and Technology of China (Grant Nos. G1999075603) and the Chinese Academy of Sciences (Grant Nos. STZ-2-07 and STZ98-2-12).

## References

Bartels, K. & Klein, C. (2000). *marFLM Version* 5.0. X-ray Research GmbH, Segeberger Chaussee 34, D-22850 Norderstedt, Germany.
Beavis, R. C. & Chait, B. T. (1990). *Anal. Chem.* **62**, 1836–1840.
Betzel, C., Lange, G., Pal, G. P., Wilson, K. S., Maelicke, A. & Saenger, W. (1991). *J. Biol. Chem.* **266**, 21530–21536.
Brown, L. R. & Würich, K. (1992). *J. Mol. Biol.* **227**, 1114–1135.
Changeux, J. P. & Edelstein, S. J. (1998). *Neuron*, **21**, 959–980.
Collaborative Computational Project, Number 4 (1994). *Acta Cryst.* D**50**, 760–763.
Corfield, P. W., Lee, T. J. & Low, B. W. (1989). *J. Biol. Chem.* **264**, 9239–9242.
Endo, T. & Tamiya, N. (1987). *Pharmacol. Ther.* **34**, 403–451.
Gaucher, J.-F., Ménez, R., Arnoux, B., Pusset, J. & Ducruix, A. (2000). *Eur. J. Biochem.* **267**, 1323–1329.
Harvey, A. L., Bradley, K. N., Cochran, S. A., Rowan, E. G., Pratt, J. A., Quillfeldt, J. A. & Jerusalinsky, D. A. (1998). *Toxicon*, **36**, 1635–1640.
Hatanaka, H., Oka, M., Kohda, D., Tate, S., Suda, A., Tamiya, N. & Inagaki, F. (1994). *J. Mol. Biol.* **240**, 155–166.
Juan, H. F., Hung, C. C., Wang, K. T. & Chiou, S. H. (1999). *Biochem. Biophys. Res. Commun.* **257**, 500–510.
Le Du, M. H., Ricciardi, A., Khayati, M., Ménez, R., Boulain, J. C., Ménez, A. & Ducancel, F. (2000). *J. Mol. Biol.* **296**, 1017–1026.
Martin, B. M., Chibber, B. A. & Maelicke, A. (1983). *J. Biol. Chem.* **258**, 8714–8722.
Martin de Llano, J. J., Jones, W., Schneider, K., Chait, B. T., Manning, J. M., Rodgers, G., Benjamin, L. J. & Weksler, B. (1993). *J. Biol. Chem.* **268**, 27004–27011.
Matthews, B. W. (1968). *J. Mol. Biol.* **33**, 491–497.
Nastopoulos, V., Kanellopoulos, P. N. & Tsernoglou, D. (1998). *Acta Cryst.* D**54**, 964–974.
Patricio, S.-B., Krauss, M., Dreger, M., Herrmann, A., Tsetlin, V. I. & Hucho, F. (1999). *Eur. J. Biochem.* **265**, 902–910.
Saludjian, P., Prangé, T., Navaza, J., Ménez, R., Guilloteau, J. P., Riès-Kautt, M. & Ducruix, A. (1992). *Acta Cryst.* B**48**, 520–531.
Smith, J. L., Corfield, P. W., Hendrickson, W. A. & Low, B. W. (1998). *Acta Cryst.* A**44**, 357–368.
Tsernoglou, D. & Petsko, G. A. (1976). *FEBS Lett.* **68**, 1–4.
Tsetlin, V. I. (1999). *Eur. J. Biochem.* **264**, 281–286.
Tsetlin, V. I., Karlsson, E., Utkin, Yu. N., Pluzhnikov, K. A., Arseniev, A. S., Surin, A. M., Kondakov, V. V., Bystrov, V. F., Ivanov, V. T. & Ovchinnikov, Yu. A. (1982). *Toxicon*, **20**, 83–93.
Tu, A. T. (1973). *Annu. Rev. Biochem.* **42**, 235–238.
Yu, C., Bhaskaran, R., Chuang, L. C. & Yang, C. C. (1993). *Biochemistry*, **32**, 2131–2136.
Zinn-Justin, S., Roumestand, C., Gilquin, B., Bontems, F., Ménez, A. & Toma, F. (1992). *Biochemistry*, **31**, 11335–11347.